Electronic structure and stability of polycrystalline cobalt clusters

R. Guirado-López, F. Aguilera-Granja, and J. M. Montejano-Carrizales
Instituto de Física "Manuel Sandoval Vallarta," Universidad Autónoma de San Luis Potosí, 78000, San Luis Potosí, Mexico
(Received 28 May 2001; revised manuscript received 23 July 2001; published 10 January 2002)

We study the electronic structure and stability of $Co_{(n+m)}$ clusters with mixed (bcc_n-fcc_m) structures [$57 \leqslant (n+m) \leqslant 177$] by means of a self-consistent tight-binding Hamiltonian solved by molecular dynamics. This type of construction is motivated by recent high-resolution transmission electron microscopy images of Co nanoparticles [Phys. Rev. B **57**, 2925 (1998)] from which the coexistence of a bcc-like crystalline arrangement with a distorted compact surface has been inferred. The minimization algorithm reveals that all the clusters undergo an inhomogeneous radial relaxation, which leads to a complex spatial distribution of the atoms within the structure. Interatomic distances which can be larger than those of bulk Co are obtained, together with a considerable surface reconstruction that favors the formation of nonplanar facets. In general, the total energy of the mixed particles increases as a function of the cluster size. However, these structures are almost in all cases less stable when compared with a pure fcc growth sequence, a fact that reveals the important role played by the polymer solution used in the stabilization of structural phases in small particles.

DOI: 10.1103/PhysRevB.65.045420 PACS number(s): 73.22.−f, 71.15.Ap, 82.70.Uv, 71.28.+d

I. INTRODUCTION

The design of new materials with novel and special desired properties is presently the subject of intense investigations.[1] Epitaxial growth technology has recently made remarkable progress. Currently it is actually possible to control the formation of new metastable and/or forced phases of matter with the desired crystal structure and lattice constant to some extent. For instance, bulk cobalt in a natural way exists in two structures depending on the pressure and temperature conditions; hcp for the low-temperature regime and fcc for the high-temperature regime.[2] However, no bcc phase has been observed spontaneously in nature. At this point we must comment that the existence of the bcc Co phase was first suggested by Prinz,[3] based on studies of Fe_xCo_{1-x} compounds in the limit of $x \to 0$. Nowadays, experimental results have shown that the bcc phase can actually be stabilized by low-temperature deposition of thin Co films (up to 2 nm) on a GaAs substrate.[4] This forced Co phase is expected to show considerably different electronic and magnetic properties when compared to the bulk ground-state structure,[5] due to the strong variations in the energy-level distribution around the Fermi energy, as well as due to the considerable distortions and bond length changes induced by the film-substrate interactions.[6]

The tailoring of structural phases has a greater degree of freedom when the dimensionality of the system is reduced, such as in ultrathin films and small clusters. This is due to the presence of finite-size effects that allow relaxation and reconstruction in the system, as a consequence stabilizing structures not permitted by classical crystallograpy rules. Although for free-standing Co clusters experimental information concerning the geometrical arrangement of the atoms is very difficult to obtain, many calculations and indirect experimental measurements (e.g., photoionization, chemical reactivity probes, and spectroscopy data) suggest that compact structures such as icosahedral and fcc (predecessors of the hcp bulk structure) are present.[7] However, when clusters are deposited on a surface or embedded in a matrix, precise structural characterizations reveal the presence of considerable geometrical transformations.[8,9] In this respect, recent high-resolution transmission electron microscopy (HRTEM) images of Co nanoparticles, synthesized by using an organometallic precursor technique, showed the existence of Co clusters consisting of a bcc-like crystalline structure surrounded by a distorted compact surface.[9] These results are similar to the ones obtained in Co thin films deposited on a GaAs(001) substrate, in which the coexistence of bcc and hcp arrangements was reported.[4] In both cases, the adopted geometrical arrangement is considerably influenced by the growth conditions, thus opening the possibility to realize metastable states of matter.

In small particles, due to the large portion of surface atoms, surface relaxation effects play an important role in determining the cluster structure. From a theoretical point of view, surface relaxation effects are difficult to quantify, the usual approach being to assume uniform contractions in all the interatomic distances in the cluster. For systems in which the coexistence of different phases is observed, not only the surface but also the interface between the different structures must be of crucial importance to determine the ground-state geometry of the particles. This is physically expected, since the local coordination number changes rapidly as we move from inner atoms to those located at the surface, allowing the existence of different interatomic forces that could lead to crystalline or amorphous types of structures. In this work, we study the structural and magnetic properties of relatively large Co particles with mixed structures, motivated by recent HRTEM images of cobalt clusters synthesized by an organometallic precursor technique.[9] We determine the ground-state configuration of our mixed particles by solving a tight-binding Hamiltonian using the method introduced by Car and Parrinello.[10] In this approach, a fictitious Lagrangian is constructed to simulate the physical trajectories of the nuclei while keeping the electrons close to their quantum ground state. The reliability of the calculations presented in this paper are supported by previous results describing the electronic and magnetic properties as well as the ground-state

structures of several transition-metal clusters.[11] In particular, predictions for the most stable geometries in small systems using this method were found to be in good agreement with those obtained by more elaborate calculations.[12]

Although the size and structure of the clusters considered in our work do not correspond to those synthesized by Respaud *et al.* (150 ± 10 and 310 ± 20 atoms),[9] our results can give us some guidelines to understand the structural and magnetic properties of these clusters with mixed structures. The rest of the paper is organized as follows. In Sec. II we describe the theoretical approach briefly. The results are presented in Sec. III, and a summary of our conclusions is given in Sec. IV.

II. MODEL

For a determination of the ground-state structures, we use a tight-binding Hubbard Hamiltonian for the d band[11,13] in the rotationally invariant form in orbital space,[14] expressed in the basis of real d orbitals of symmetry t_{2g} (xy, yz, zx) and e_g (x^2-y^2, $3z^2-r^2$). In this basis the most important matrix elements of the on-site Coulomb interaction, i.e., involving one or two orbitals, are intraorbital ($U+2J$) and interorbital (U) Coulomb and exchange (J) integrals. The electronic structure of the clusters is determined by solving this model with the interactions treated in the Hartree-Fock approximation (HFA). Using the basis of $3d$ atomic spin-orbitals $|i\lambda\sigma\rangle$ centered at each site i, one finds[11,13]

$$H_{\mathrm{HFA}}=\sum_{i\lambda,\sigma}\epsilon_{i\lambda\sigma}n_{i\lambda\sigma}+\sum_{i,\lambda,\mu\neq\lambda,\sigma}h_{i,\lambda\mu,\sigma}c^{+}_{i\lambda\sigma}c_{i\mu\sigma}+\sum_{i\lambda,j\mu,i\neq j,\sigma}t_{i\lambda,j\mu}c^{+}_{i\lambda\sigma}c_{j\mu\sigma}, \tag{1}$$

in the usual notation. The on-site energy levels $\epsilon_{i\lambda\sigma}$ are given in terms of the spin-orbital occupation numbers $\langle n_{i\lambda\sigma}\rangle$ and electron-electron interactions as

$$\epsilon_{i\lambda\sigma}=\epsilon_d^o+(U-\tfrac{1}{2}J)[N(i)-N_a]-\tfrac{1}{2}(U-3J)(\langle n_{i\lambda}\rangle-n_a)-\tfrac{1}{2}\sigma JM(i)-\tfrac{1}{2}\sigma(U+J)\langle m_{i\lambda}\rangle, \tag{2}$$

where σ is the spin index ($\sigma=\pm1$). Here we have introduced the occupation number $\langle n_{i\lambda}\rangle=\langle n_{i\lambda\uparrow}\rangle+\langle n_{i\lambda\downarrow}\rangle$ and the magnetic moment $\langle m_{i\lambda}\rangle=\langle n_{i\lambda\uparrow}\rangle-\langle n_{i\lambda\downarrow}\rangle$ of each orbital λ. $N(i)$ and $M(i)$ are the total number of electrons and the total magnetic moment at atom i, respectively.

The second term in Eq. (1) corresponds to the intrasite interorbital Fock terms ($\bar{\sigma}=-\sigma$)

$$h_{i,\lambda\mu,\sigma}=(J-U)\langle c^{+}_{i\mu,\sigma}c_{i\lambda,\sigma}\rangle+2J\langle c^{+}_{i\mu,\bar{\sigma}}c_{i\lambda,\bar{\sigma}}\rangle. \tag{3}$$

They vanish in the bulk for symmetry reasons. Finally, the hopping integrals $t_{i\lambda,j\mu}$ are obtained in the Slater-Koster scheme[15] from the parameters $(dd\sigma)$, $(dd\pi)$, and $(dd\delta)$. We have carried out a least mean-square fit of the bulk levels which correspond to a wave function of pure d character calculated within the local-density-approximation formalism using only two parameters $(dd\sigma_0)$ and $(dd\pi_0)$, since $(dd\delta_0)$ is very small and can be neglected. As usual, these parameters are assumed to vary with the distance R_{ij} between atoms i and j as ($\lambda=\sigma,\pi,\delta$)

$$dd\lambda=dd\lambda_0\exp[-q(R_{ij}/R_0-1)], \tag{4}$$

where R_0 is the bulk interatomic spacing. In the calculations, orbitals located on first- and second-nearest-neighbor atoms are included.

TABLE I. Hopping parameters $(dd\sigma_o)$ and $(dd\pi_o)$, and electron-electron interaction parameters: U and J (all in eV) estimated for bulk Co.

	$(dd\sigma_o)$	$(dd\pi_o)$	U	J
Co	−0.5800	0.2900	1.3	0.76

The bond length and the magnetic states of the clusters are determined by minimizing the total energy,

$$E_{\mathrm{tot}}(N)=\langle H_{\mathrm{HFA}}\rangle-\langle H_{\mathrm{int,HFA}}\rangle+E_{\mathrm{rep}}, \tag{5}$$

where $\langle H_{\mathrm{int,HFA}}\rangle$ refers to the double counting correction,[13] and the repulsive energy E_{rep} is of the Born-Mayer type, i.e., it is described by a sum of pair interaction energies:

$$A(R_{ij})=A_0\exp[-p(R_{ij}/R_0-1)], \tag{6}$$

between first nearest neighbors. The corresponding parameters of the model shown in Tables I and II are obtained from bulk properties: cohesive energy, bulk modulus, bandwidth, and equilibrium distance.[13]

The total energy E_{tot} can be considered as a function of both (i) the set of ion coordinates $\{\mathbf{R}_i\}$ and (ii) the set of components $\{c^{(n)}_{i\lambda\sigma}\}$ of the occupied eigenstates in the atomic orbital basis set, and has to be minimized with respect to all these variables in order to find the ground state of the cluster. This is carried out using the Born-Oppenheimer approximation, i.e., at any position of the ions $\{\mathbf{R}_i\}$, E_{tot} should be at its minimum with respect to $\{c^{(n)}_{i\lambda\sigma}\}$. In principle, this can be achieved by a self-consistent diagonalization of the Hamiltonian at each atomic configuration $\{\mathbf{R}_i\}$. Then the force acting on each ion can be computed, and the positions $\{\mathbf{R}_i\}$ are updated according to classical dynamics until all forces vanish. However, this procedure would be very time consuming, and we have preferred to use the fictitious Lagrangian method.[10,13,16] This method provides an equation of motion for the components $\{c^{(n)}_{i\lambda\sigma}\}$, thus avoiding the self-consistent diagonalization of the Hamiltonian at each step.

The dynamics of the system is thus governed by the equations

TABLE II. Number of d electrons per atom N_d, equilibrium interatomic distance in the bulk R_o, hopping integral exponent q, and the parameters of the pair repulsive potential, A_o and p, for bulk Co.

	N_d	R_o (Å)	q	A_o (meV)	p
Co	8.0	2.446	3.09	159.3	9.12

$$M\ddot{R}_{i\gamma} = -\frac{\partial E_{\rm tot}(\{c_{i\alpha\sigma}^{(n)}\},\{\mathbf{R}_i\})}{\partial R_{i\gamma}} \tag{7}$$

for the ions, with $\gamma = x,y,z$, and

$$\mu\ddot{c}_{i\alpha\sigma}^{(n)} = -\frac{\partial E_{\rm tot}(\{c_{i\alpha\sigma}^{(n)}\},\{\mathbf{R}_i\})}{\partial c_{i\alpha\sigma}^{(n)}} + \sum_{n'} \Lambda_\sigma^{nn'} c_{i\alpha\sigma}^{(n')} \tag{8}$$

for fictitious particles (here n and n' are occupied electronic states). The quantities $\Lambda_\sigma^{nn'}$ are Lagrange multipliers defined as

$$\Lambda_\sigma^{nn'} = \sum_{i\alpha}\left[\frac{1}{2}\frac{\partial E_{\rm tot}}{\partial c_{i\alpha\sigma}^{(n)}}c_{i\alpha\sigma}^{(n')} + \frac{1}{2}c_{i\alpha\sigma}^{(n)}\frac{\partial E_{\rm tot}}{\partial c_{i\alpha\sigma}^{(n)}} - \mu\dot{c}_{i\alpha\sigma}^{(n)}\dot{c}_{i\alpha\sigma}^{(n')}\right]. \tag{9}$$

The above equations of motion are integrated numerically using the Verlet algorithm.[17] For more details the reader is referred to Refs. 11, 13, and 16.

III. RESULTS AND DISCUSSION

A. Cluster geometries

For the calculations we have considered $Co_{(n+m)}$ clusters of different sizes (where n corresponds to atoms with a bcc structure and m specifies those having a fcc arrangement) within the following range: $57 \leqslant (n+m) \leqslant 177$. The particles consist of a growing bcc core ($n=9,15,27$) embedded by subsequent fcc layers (up to six) having $48 \leqslant m \leqslant 150$ atoms, which are enough to completely cover the inner bcc structures. In Fig. 1, we show as representative examples the initial atomic configurations for Co_{69} ($n=15,m=54$) [Fig. 1(a)], Co_{93} ($n=15,m=78$) [Fig. 1(b)], and Co_{105} ($n=27,m=78$) [Fig. 1(c)] clusters. Obviously, this type of construction originates an abrupt interface between the embedded core and the external fcc layers that, as will be seen in the following, is of fundamental importance in determining the electronic properties and stability of the particles. It is important to comment that this kind of interface could be present in systems where the coexistence between different geometrical phases was reported, such as in small Cobalt nanoparticles[9] and thin Co films deposited on GaAs(001).[4]

As an input for the relaxation procedure we will consider that all the nearest-neighbor distances within the clusters are the same and equal to the bulk Co hcp value ($R_0 = 2.48$ Å). However, such a restriction is removed as the minimization process evolves. In this algorithm, a purely radial dependence of the atomic positions will be considered, thus avoiding any deviation from the initial symmetry of the particle. The structural relaxations of our optimized geometries will be then analyzed in terms of the relaxation of the layers in the clusters, i.e., in terms of the distance of all other atoms from the central atom. Despite the fact that angular distortions must be also included, our symmetry-constrained minimization procedure could be justified since, as previously stated, HRTEM images of Co nanoparticles embedded in a polymer matrix have revealed that local order for cobalt in these particles is not the same for the core and surface; the former being characterized by the presence of square lattices with interatomic distances corresponding to those of a bcc arrangement, while the latter is formed by a distribution of distances close to those of a close-packed arrangement.

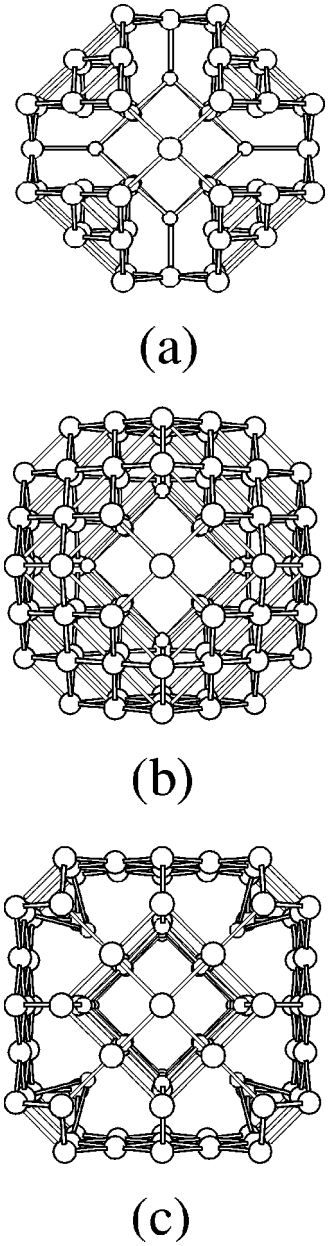

FIG. 1. Illustration of the initial atomic configurations for (a) Co_{69} ($n=15$, $m=54$), (b) Co_{93} ($n=15$, $m=78$), and (c) Co_{105} ($n=27$, $m=78$).

B. Relaxed structures and total energy

To illustrate the complex pattern of interatomic distances that occurs in our mixed particles upon optimization, we first show in Fig. 2 the distances from the central atom ($j=0$) to each one of the neighbor shells (j), R_{0j}, for three different nonmagnetic Co clusters [i.e., by assuming in Eq. (1) that $J=0$ and $\langle n_{i\alpha\uparrow}\rangle = \langle n_{i\alpha\downarrow}\rangle$ in all cases], with different bcc core sizes ($n=9,15,27$). Together with this radial distance distri-

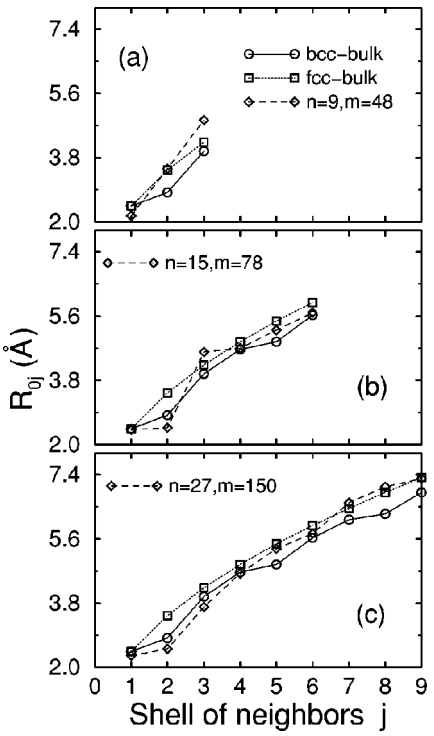

FIG. 2. The relaxation of each one of the atomic shells (j) with respect to the central atom ($j=0$), R_{0j}, for nonmagnetic (a) Co_{57} ($n=9$, $m=48$), (b) Co_{93} ($n=15$, $m=78$), and (c) Co_{177} ($n=27$, $m=150$) clusters. In all cases, the ratio of bcc to fcc atoms is ~ 0.2. For comparison, the interatomic spacing of unrelaxed terminated fcc and bcc bulk fragments are also included.

bution we also plot, for comparison, the interatomic spacing of unrelaxed terminated fcc and bcc bulk clusters. In order to reduce the number of free parameters and simplify the discussion, all the clusters in Fig. 2 have ratio of bcc to fcc atoms of ~ 0.2. From the figure we can see that the ground-state configuration in all the particles is achieved by sizable changes in the positions of the atomic shells with respect to the bulk. Considerable contractions and expansions are both present, the latter mainly localized at the interface [Fig. 2(b)] and at the outermost layers of the particles [Figs. 2(a) and 2(c)]. In all cases, note that rather large average compressions on the embedded bcc clusters are observed. At this point we must comment that it is generally believed that an atom can largely compensate for a coordination deficit by reducing its interatomic distances. However, as can be seen from the figures, close-packed atomic distributions (external layers) can also suffer considerable expansions and contractions (although more modest), showing that maximizing the average coordination may not generate the optimal structure in all cases. Obviously, the atomic reconstructions observed in the figures are more complex than the ones obtained in extended surfaces and, as a consequence, surfaces with unique reactive properties should be expected in these particles.

As is well known, as a function of the number and coordination of surface atoms, different structural rearrangements for the external layers are possible, being the cause of a geometrical perturbation that propagates into the inner shells and which produces a complex nonuniform relaxation profile within the particles.[11] However, as previously stated, in systems where different geometrical phases coexist, not only the surface but the presence of an interface should play a major role in the determination of the ground-state structure. Interface effects are clearly illustrated in Fig. 2(b), where we show the radial distance distribution for a Co_{93} cluster with a 15-atom bcc core. In this case, we note that the last shell of the embedded bcc cluster ($j=2$) and the first layer of the fcc arrangement ($j=3$), which form the bcc-fcc interface in this particle, suffer a considerable repulsive relaxation which obviously causes a redistribution of the neighboring shells. Note that the atoms belonging to $j=1$ and 2 of the bcc core are practically located at the same distance from the center of the particle (a relaxation process not present in the free-standing bcc Co_{15} cluster), so that the central atom becomes a highly coordinated site with 14 first-nearest neighbors. The collapse of atomic shells in Fig. 2(b) is also observed between $j=3$ and 4 (the first two layers of the fcc structure), which leads to the formation of a sizable cavity within the cluster. This type of atomic relaxation can be at the origin of the formation of radial regions of low (high) atom concentration in the radial distribution function (RDF), such as the ones observed in Ref. 9. At this point it is important to comment that the contribution of the sp electrons has been omitted in the electronic model; as a consequence, the bond length changes presented in the the figures may not be very accurate (see Fig. 5 of Ref. 11). However, we expect that the rather complex size and environment dependence obtained for the radial distance distribution should reflect the realistic situation in this kind of system.

In order to furthermore elucidate the structural relaxations present in this type of mixed structures, in Fig. 3 we compare the interatomic distance distribution (R_{0j}) [Fig. 3(a)] as well as the RDF [Fig. 3(b)] for a mixed Co_{177} particle with the ones obtained for an optimized fcc Co_{165} cluster. Despite the fact that both structures differ in the total number of atoms, the number of atomic shells that surround the central Co atom are the same ($j=9$), a fact that could be useful to quantify the influence of the coexistence of different packings in the particles. From the figures we can observe significant variations between both clusters in R_{0j} and the RDF as a consequence of the sizable differences in their local atomic environment. Our calculations for the fcc cluster reveal that the largest contractions are limited to surface layers, while an almost bulklike distribution can be observed for those atoms located at the inner shells of the particle [Fig. 3(a)]. These results are in agreement with experimental observations in transition-metal surfaces in which a noticeable contraction of the first layer has been found, followed by a damped oscillation of the interlayer spacing around the bulk values when going into the crystal. On the other hand, note that for a mixed Co_{177} structure, strong variations in the local coordination number as well as interface and surface effects are combined to generate a complex nonuniform relaxation profile. By looking at Fig. 3(a) we can see that, as in previous cases, the distance between the atomic shells with $j=1$ and 2 is very small, a fact that is reflected in the RDF [Fig. 3(b)] by the formation of a small shoulder in the largest peak

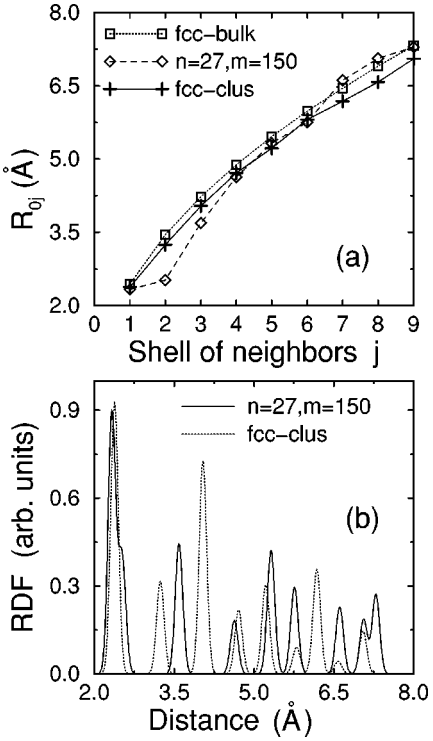

FIG. 3. (a) The relaxation of each one of the atomic shells (j) with respect to the central atom ($j=0$), R_{0j}, for the nonmagnetic Co_{177} ($n=27$, $m=150$) cluster compared with the distribution obtained for a relaxed and unrelaxed fcc bulk fragment. In (b) the radial distribution function (RDF) for Co_{177} in comparison with the one found for an optimized fcc Co_{165} cluster.

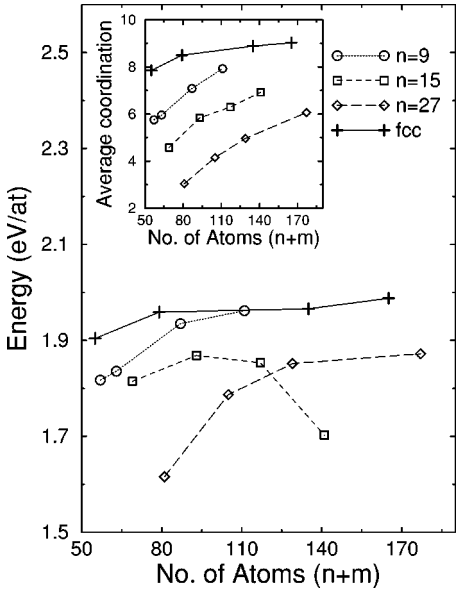

FIG. 4. Size dependence of the binding energies per atom for Co clusters at their ground-state geometrical configuration: solid line, pure fcc relaxed structures; dotted line, mixed growth sequence with $n=9$; dashed line, mixed growth sequence with $n=15$; long-dashed line, mixed growth sequence with $n=27$. In the inset we show the respective size dependence of the average coordination number.

of the distribution centered around 2.3 Å. Moreover, also note that, in this case, the relaxation of the bcc-fcc interface ($j=3$ and 4) causes the formation of sizable cavities within the structure, the location of the peaks in the pure fcc cluster being more uniformly distributed in space.

We have also calculated the total-energies of our mixed particles at $T=0$ by using the tight-binding total energy expression [Eq. (5)] given in Sec. II. The size dependence of the binding energy per atom for all nonmagnetic ($J=0$ and $\langle n_{i\alpha\uparrow}\rangle=\langle n_{i\alpha\downarrow}\rangle$) free-standing Co clusters considered in the calculations, at their ground state, is shown in Fig. 4. Three mixed bcc_n-fcc_m growth sequences are considered with different bcc cores: $n=9$, 15, and 27. For comparison, the binding energy of pure fcc relaxed structures (Co_{55}, Co_{79}, Co_{135}, and Co_{165}) is also shown. From the figure we note that, in general, mixed structures are found to be less stable when compared to fcc clusters. However, note that for particles with $(n+m)=87$ and 111, which corresponds to the largest Co structures with a nine-atom bcc core, the calculated binding energies are very close to those of the pure fcc growth sequence, showing the behavior of the local impurity limit due to the small fraction of bcc atoms ($\sim 10\%$) present in the clusters. From the figure we note that, for fcc structures, the binding energy increases as the number of atoms in the particles increases, reaching almost an asymptotic value of 1.96 eV/at for ~ 170 atoms. The same kind of behavior is obtained for mixed structures with nine and 27 bcc cores, whereas for the mixed growth sequence with $n=15$ a parabolic dependence for the energy is obtained, the maximum value being located at $(n+m)=93$.

It is important to comment that, in almost all cases, the size dependence of the binding energy can be correlated with the average coordination number of the clusters, $\langle z\rangle$. This is clearly seen in the inset of Fig. 4, where the average coordination as a function of the number of atoms in the particles is shown. Note that, for pure fcc clusters as well as for the mixed particles with $n=9$ and 27, a monotonically increasing behavior is observed in both binding energy and $\langle z\rangle$. Moreover, following simple geometrical arguments, we observe that the more compact structures are in general the most stable ones. In contrast, it is important to remark that the total coordination count cannot explain the binding energy vs $(n+m)$ curve for $n=15$; the former increases with size while the latter considerably decreases. In this particular case, electronic effects play an important role in the observed decreasing behavior of the energy profile. As is well known, clusters with a large energy gap between the highest occupied molecular orbital (HOMO) and the lowest unoccupied molecular orbital (LUMO) are expected to show remarkable stability; as a consequence, in Fig. 5 we plot the HOMO and the LUMO as functions of cluster size. From the figure we can see that the relative stability observed in Fig. 4 can also be correlated to some extent with the HOMO-LUMO energy separation of the particles. Note that the largest HOMO-LUMO energy differences correspond in almost all cases to the pure fcc arrangements which are the most stable of all the considered structures. Moreover, note that for the growth sequence with $n=15$, the smallest HOMO-LUMO energy gap

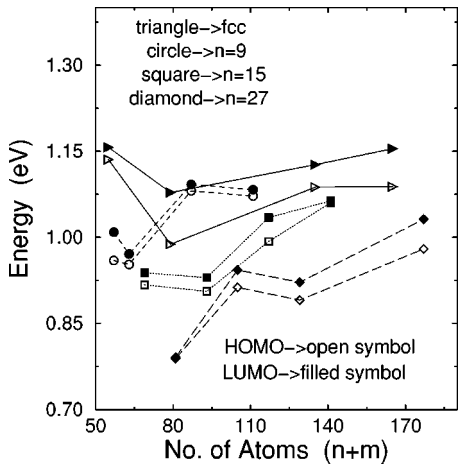

FIG. 5. Size dependence of the HOMO (open symbols) and LUMO (filled symbols) for all Co clusters considered in the calculations at their ground state.

(0.003 eV) is found for the largest particle of the distribution (Co_{141}), an energy ordering that agrees with the one obtained for the binding energies in Fig. 4. As is well known, this small HOMO-LUMO energy difference will result in a large value for the density of states at the Fermi level E_F, a fact that will tend to distort the structure further toward a lower symmetry arrangement (according to the Jahn-Teller theorem) in order to reduce the degeneracy around E_F and lower the total energy. Obviously, our symmetry-constrained minimization procedure does not allow such structural transformations; however, as will be seen in the following, the inclusion of magnetic effects will induce further atomic reconstructions in the clusters, accompanied by considerable energy gains, thus enhancing the stability of the particles. From these results we can conclude that, as physically expected, the energetics and structural rearrangements presented in Figs. 2, 3, and 4 result from a delicate balance between the electronic and geometrical details present in the particles.

Though our total-energy calculations reveal that in the free-standing case these mixed clusters are less favorable when compared with the fcc structures, the fact that they have been synthesized in a colloidal suspension shows the important role played by the polymer solution in the stabilization of these kind of arrangements. At this point, it is important to comment that recently Garzon *et al.*[18] found that disordered ground-state structures are obtained for gold clusters when passivated with organic molecules. Similarly, in the case of the cobalt nanoparticles synthesized by Respaud *et al.*,[9] the interaction of the Co cluster surface with the ligand molecules or fragments could play also a major role in the observed geometrical configuration and stability of these type of nanoparticles.

Up to this stage we have not considered the well-known presence of magnetic order in Co particles. In previous theoretical calculations[19] and experimental measurements[9,20] the existence of enhanced magnetic moments with respect to the bulk Co structure was reported. Moreover, as is well known, the lattice constant of clusters[21] and bulk[22] transition metals are larger in magnetic states than in nonmagnetic states, and therefore are of interest when investigating the dependence of our relaxation profiles and binding energies on the total magnetization of our clusters. We have thus also performed spin-polarized calculations by means of the full ($U \neq 0, J \neq 0$) extended multiband Hubbard Hamiltonian presented in Sec. II. Moreover, we have explored the existence of multiple magnetic solutions by changing our initial spin-polarized electronic configuration in our self-consistent diagonalization process. These multiple magnetic solutions correspond to local minima of the total energy as a function of the magnetic moment of the system for a given geometry, among which the one that gives the lowest total energy is regarded as the ground state of the cluster; the rest, with higher energies, are only metastable states.

The magnetic ground states in all our clusters (mixed and pure) have been found to be fully polarized, the average magnetic moment per atom $\langle M \rangle$ being equal to $2\mu_B$. This is actually due to the fact that the large exchange interaction J (see Table I) dominates independently of the assumed geometrical configuration; thus very similar distribution of the local magnetic moments $M(j)$ are found in all cases. Our estimated values for $\langle M \rangle$ are in good agreement with the experimental findings of Ref. 9, where the mean magnetic moment of Co nanoparticles containing 150 ± 10 and 310 ± 20 atoms is $\sim 2.0\mu_B$. Our calculations also agree with the experimetal results of Douglass *et al.*[23] who found that for free Co clusters with sizes ranging from 56 to 215 atoms the average magnetic moment per atom is $1.96\mu_B \pm 0.12\mu_B$. In addition to the fully polarized state, several intermediate values of magnetizations have also been obtained, being less stable and characterized by a complicated distribution of the local magnetic moments within the particles with both ferromagnetic and antiferromagnetic configurations. This is in contrast to the local-moment distribution obtained for a fully polarized state in which all moments are of course ferromagnetically aligned and only small fluctuations in $|M(j)|$ are observed with respect to average value ($\langle M \rangle = 2.0\mu_B$) of the clusters.

At this point, it is important to comment that, even though the exchange parameter J plays the most important role in determining the magnetism of transition-metal clusters,[24] the correlation between the on-site Coulomb interaction and the local charge fluctuations also gives a certain dependence of the magnetic states on the value of U. As is well known, low values of this parameter favor a sizable spin-polarized charge transfer between geometrically inequivalent sites which obviously could modify the distribution of the local magnetic moments in the particles. Although in a previous publication[11] it was demonstrated that sizable variations in the Coulomb interaction do not induce significant perturbations on the relaxation profiles of relatively large nonmagnetic clusters, in the present case it is important to analyze whether fluctuations in the local magnetic moments induced by the local fluctuations of charge could modify the details of the radial distance distributions. Consequently, in order to check the sensitivity of our results with the value of the on-site Coulomb interaction, we have performed additional calculations by considering different values of U. In Fig. 6

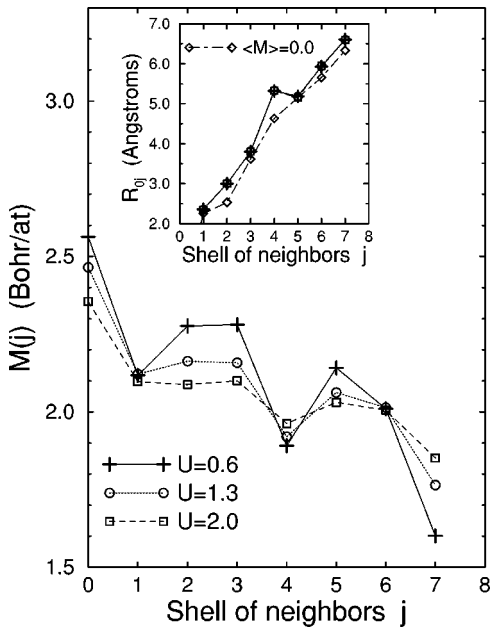

FIG. 6. The distribution of the local magnetic moments for the mixed fully polarized Co_{105} ($n=27$, $m=78$) cluster for three different values of the on-site Coulomb interaction U. In the inset, we show the respective relaxation profiles.

we plot the magnetic moments on atoms of the jth shell of neighbors, $M(j)$, for a mixed Co_{105} cluster for $U=0.6$, 1.3, and 2.0 eV. We only show the most stable solution found for each U, which corresponds in all cases to the fully polarized state $\langle M\rangle=2.0\mu_B$. Moreover, in the inset we also plot the respective results for the radial distance distribution R_{0j}. From the figure it is clear that a lower value of U (0.6 eV) than the one considered in our work (see Table I) increases the electron delocalization in the system and, despite the fact that the same general shape of the $M(j)$ vs j curve is obtained, sizable variations in the magnitude of the local magnetic moments are observed in almost all atoms in the particle. Conversely, higher values of U (2.0 eV) enhance the electron localization, and thus produce a less anisotropic distribution of the local magnetic moments in the structure.

Note that, in all three cases, the largest deviations from the average value $\langle M\rangle=2.0\mu_B$ are always observed at $j=0$ and at the surface of the particle. In the first case this is due to the fact that the perturbation introduced by the surface of the cluster is symmetric around the atom in the center, and therefore produces very strong changes in its local density of states, causing strong oscillations in the value of $M(j=0)$. For the atoms at the surface, a small charge transfer ($\sim 0.2\bar{e}$/at) from the core atoms to those located at the outermost layers, resulting mainly from the different effective bandwidth of the local density of states, causes the minority-spin states to become more filled, lowering the value of $M(j)$ at those sites as a consequence. The influence of magnetic effects on the relaxation profiles are clearly illustrated in the inset of the figure, where we show the radial distance distribution for a mixed fully polarized Co_{105} cluster obtained for the three considered values of U. For comparison, we also show the relaxation profile obtained for the same

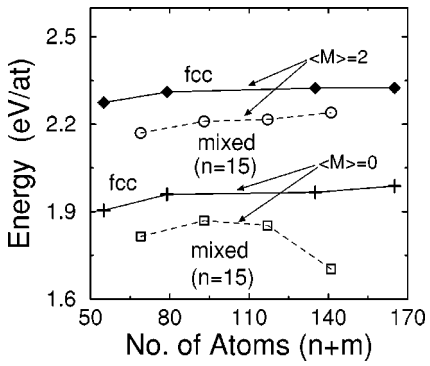

FIG. 7. A comparison of the size dependence of the binding energies per atom for Co clusters at their nonmagnetic and magnetic ground state: filled diamonds, magnetic fcc growth; open circles, nonmagnetic fcc growth; crosses, magnetic mixed growth with $n=15$; open squares, nonmagnetic mixed growth with $n=15$.

cluster in a nonmagnetic state. Note that the presence of magnetic order modifies the positions of all atomic shells significantly with respect to the results with $\langle M\rangle=0$; the expansive relaxation at the interface (between $j=3$ and 4) and at the outermost layers is now more pronounced. Moreover, note that changing the value of the Coulomb interaction U does not induce appreciable modifications in the radial distance relaxation profile, the ground-state geometry of the fully polarized state being almost independent of the local distribution of the magnetic moments in the structure.

The energy contributions of the spin-dependent terms in Eq. (2) are also of fundamental importance in determining the stability of this nanoparticles. In Fig. 7, as a representative example we show a comparison of the binding energies obtained for two growth sequences (mixed with $n=15$ and pure fcc) in their magnetic and nonmagnetic states. From the figure it is clear that the magnetic contributions produce an almost rigid energy shift of ~ 0.2 eV/at on the values obtained in the nonmagnetic fcc growth, while for a mixed sequence with $n=15$ sizable changes in the general shape of the energy profile are observed. Actually, it is important to remark that, with the inclusion of magnetic effects, the energy vs $(n+m)$ curve for $n=15$ now shows a monotonically increasing behavior (compare Figs. 4 and 7), a fact that clearly demonstrates how the presence of magnetism seems to be also a key factor for stabilizing this type of mixed structure.

In order to obtain a clearer picture on the type of surface relaxations present in the clusters, in Fig. 8 we show the ground-state atomic configuration for Co_{69} [Fig. 8(a)], Co_{93} [Fig. 8(b)], and Co_{105} [Fig. 8(c)] particles in their nonmagnetic (left column) and magnetic (right column) ground states. Despite the complex radial distance distribution obtained upon optimization, we can see that, if we compare the initial configurations of the clusters (Fig. 1) with their corresponding nonmagnetic ground-state geometries (left column of Fig. 8), no striking differences are found in the general morphology of the particles. However, note that with the inclusion of magnetic effects (right column of Fig. 8), additional geometrical reconstructions occur, as the atoms located in the center of the fcc faces contract differently than

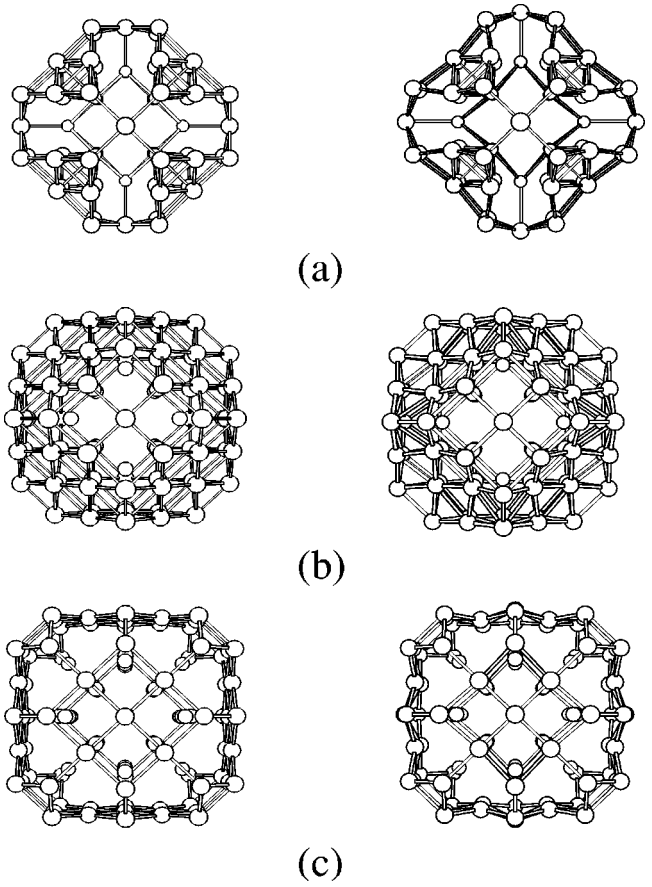

FIG. 8. Illustration of the nonmagnetic (left column) and magnetic (right column) ground-state atomic configurations for (a) Co_{69} ($n=15$, $m=54$), (b) Co_{93} ($n=15$, $m=78$), and (c) Co_{105} ($n=27$, $m=78$).

those located at the corners, resulting in a ''puckered'' type of structure with obviously unique reactive properties. Actually, for larger particles, this effect will become less pronounced for the atomic shells located near the center of the structure; however, the outer layers are expected to exhibit similar features. At this point, it is important to comment that this kind of surface reconstruction is absent in pure fcc clusters, a fact that clearly shows the close interdependence of magnetism and cluster geometry, and how the magnetic ordering can affect the atomic configuration of a given structure.

Finally, it is important to comment upon a few limitations of our model. As already discussed in Sec. II, the tight-binding model describes only $3d$ electrons and neglects sp electrons and sp-d hybridization effects. With respect to magnetic properties, it is well known that s and p electrons have small magnetic moments which are normally antiferromagnetically alligned with respect to those in the d orbitals, thus causing a small reduction in the total magnetic moment of the clusters. On the other hand, sp electrons are important because they fix the number of d electrons in the d band by means of sp-d hybridization. Actually, within our theoretical framework, trends for sp-d charge transfers can be inferred by varying the d-electron occupancy around the value considered in our work, $N_d=8.0$. To see this, in Fig. 9 we show

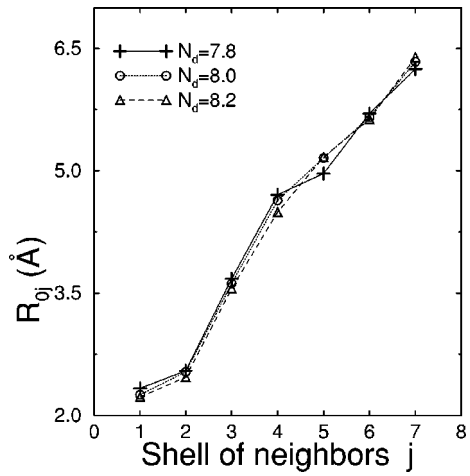

FIG. 9. A comparison of the radial distance distribution R_{0j} for the mixed nonmagnetic Co_{105} cluster for different values of the d-band filling.

additional calculations for a mixed Co_{105} cluster by considering $N_d=7.8$, 8.0, and 8.2. From the figure, it is clear that sizable variations in the d-electron occupancy around $N_d=8.0$ only induces minor modifications on the general shape of the relaxation profile; as a consequence, we believe that no erroneous conclusions are given in our work, despite the unknown occupancy of the d states in all the considered structures.

IV. SUMMARY AND CONCLUSIONS

Using the tight-binding total-energy formalism together with molecular-dynamics techniques, we have performed calculations on the structure and total energies of relatively large sized $Co_{(n+m)}$ clusters with mixed (bcc_n-fcc_m) structures. These particles are characterized by small bcc clusters that have been covered with several fcc layers in order to simulate the geometrical structure of cobalt nanoparticles recently synthesized by an organometallic precursor technique. The relaxation of the atoms forming the bcc-fcc interface together with surface relaxations effects were found to be of fundamental importance in determining the electronic structure and ground-state geometries of the clusters. In all cases we obtained complex nonuniform distributions of the atomic shells within the clusters, characterized by sizable contractions and expansions with respect to the bulk. The formation of sizable cavities in the particles as well as asymmetrically broadened peaks in the radial distribution function was observed, being in qualitative agreement with the experimental atomic distribution measured by Respaud *et al.*[9] Our mixed structures were found to be generally less stable when compared with pure fcc arrangements, a fact that clearly shows the crucial role played by the polymer solution in the stabilization of these kind of nanoparticles. Small HOMO-LUMO energy gaps were obtained in all cases, indicating a metalliclike behavior in the clusters. In agreement with previous theoretical calculations and experiments, we have found fully polarized magnetic ground states ($\langle M\rangle = 2.0\mu_B$) in all particles. Actually, the presence of magne-

tism in the clusters was found to play a key role for the stability of this kind of arrangement by inducing more favorable atomic reconstructions, as well as due to the sizable energy contributions of the spin-dependent terms taken into account in the electronic Hamiltonian.

The results presented in this paper can be considered as a first step in the study of electronic, structural, and magnetic properties of these nanoparticles with mixed structures, since here we have concentrated on qualitative trends rather than on accurate descriptions of particular systems. The main advantage of the considered tight-binding model is its simplicity, that allowed us to obtain a physical insight into the nature of the complex structural transformations present in cobalt clusters with mixed structures, as well as to elucidate the possible geometrical and electronic features responsible for their stability.

We would like to acknowledge the financial support by CONACyT, México, for the Grants J32084-E and G25851-E. Two of us (F.A.G. and J.M.M.C.) also acknowledge the partial support of the Milleniun Iniciative (CONACyT) through the Grant W-8001. Finally FAG also acknowledges the FONDECyT (7010511), Chile, for partial support.

[1] L. M. Falicov, D. T. Pierce, S. D. Bader, R. Grosky, K. B. Hathaway, H. J. Hopster, D. N. Lambert, S. P. Parkin, G. Prinz, M. Salomon, I. K. Schuller, and R. H. Victora, J. Mater. Res. **5**, 1299 (1990).

[2] C. Kittel, *Introduction to the Solid State Physics* (Wiley, New York, 1975).

[3] G. A. Prinz, Phys. Rev. Lett. **54**, 1051 (1985).

[4] Y. U. Idzerda, W. T. Elam, B. T. Jonker, and G. A. Prinz, Phys. Rev. Lett. **62**, 2480 (1989); Y. Z. Wu, H. F. Ding, C. Jing, D. Wu, G. L. Liu, V. Gordon, G. S. Dong, X. F. Jin, S. Zhu, and K. Sun, Phys. Rev. B **57**, 11 935 (1998).

[5] P. M. Marcus and V. L. Moruzzi, Solid State Commun. **55**, 971 (1985).

[6] A. Rabe, N. Memmel, A. Steltenpohl, and Th. Fauster, Phys. Rev. Lett. **73**, 2728 (1994).

[7] M. Pellarin, B. Baguenard, J. L. Vialle, J. Lermé, M. Broyer, J. Miller, and A. Perez, Chem. Phys. Lett. **217**, 349 (1994); M. Pellarin, B. Baguenard, M. Broyer, J. E. Lermé, J. L. Vialle, and A. Pérez, J. Chem. Phys. **98**, 944 (1993); E. K. Parks, T. D. Klots, B. J. Winter, and S. J. Riley, *ibid.* **95**, 8919 (1991); **99**, 5831 (1993).

[8] O. Kitakami, H. Sato, Y. Shimada, F. Sato, and M. Tanaka, Phys. Rev. B **56**, 13 849 (1997).

[9] M. Respaud, J. M. Broto, H. Rakoto, A. R. Fert, L. Thomas, B. Barbara, M. Verelst, E. Snoeck, P. Lecante, A. Mosset, J. Osuna, T. Ould Ely, C. Amiens, and B. Chaudret, Phys. Rev. B **57**, 2925 (1998).

[10] R. Car and M. Parrinello, Phys. Rev. Lett. **55**, 2471 (1985); **60**, 204 (1988).

[11] B. Piveteau, M. C. Desjonquères, A. Oleś, and D. Spanjaard, Phys. Rev. B **53**, 9251 (1996); R. Guirado-López, D. Spanjaard, and M. C. Desjonquères, *ibid.* **57**, 6305 (1998); C. Barreteau, D. Spanjaard, and M. C. Desjonquères, *ibid.* **58**, 9721 (1998); C. Barreteau, R. Guirado-López, D. Spanjaard, M. C. Desjonquères, and A. Oleś, *ibid.* **61**, 7781 (2000); R. Guirado-López, M. C. Desjonquères, and D. Spanjaard, *ibid.* **62**, 13 188 (2000); R. Guirado-López, *ibid.* **63**, 174420 (2001).

[12] D. R. Jennison, P. A. Schultz, and M. P. Sears, J. Chem. Phys. **106**, 1856 (1997).

[13] B. Piveteau, M. C. Desjonquères, A. M. Oleś, and D. Spanjaard, Phys. Rev. B **53**, 9251 (1996).

[14] A. M. Oleś, Phys. Rev. B **28**, 327 (1983).

[15] J. C. Slater and G. F. Koster, Phys. Rev. **94**, 1498 (1954).

[16] F. S. Khan and J. Q. Broughton, Phys. Rev. B **39**, 3688 (1989); **43**, 11 754 (1991).

[17] L. Verlet, Phys. Rev. **159**, 98 (1967).

[18] I. L. Garzón, C. Rovira, K. Michaelian, M. R. Beltran, P. Ordejon, J. Junquera, D. Sanchez-Portal, E. Artacho, and J. M. Soler, Phys. Rev. Lett. **85**, 5250 (2000).

[19] J. Guevara, F. Parisi, A. M. Llois, and M. Weissmann, Phys. Rev. B **55**, 13 283 (1997); A. N. Andriotis and M. Menon, *ibid.* **57**, 10 069 (1998); J. Guevarra, A. M. Llois, F. Aguilera-Granja, and J. M. Montejano-Carrizales, Solid State Commun. **111**, 335 (1999).

[20] I. M. Billas, A. Châterline, and W. A. de Heer, Science **265**, 1682 (1994).

[21] G. Pastor, J. Dorantes-Dávila, and K. H. Benemann, Phys. Rev. B **40**, 7642 (1989).

[22] V. L. Moruzzi, J. F. Janak, and A. R. Williams, *Calculated Electronic Properties of Metals* (Pergamon, New York, 1978).

[23] D. C. Douglass, A. J. Cox, J. P. Bucher, and L. A. Bloomfield, Phys. Rev. B **47**, 12 874 (1993).

[24] J. Dorantes-Dávila, H. Dreyssé, and G. M. Pastor, Phys. Rev. B **46**, 10 432 (1992).